Redox Homeostasis

Deutsche Ausgabe: DOI: 10.1002/ange.201601026
Internationale Ausgabe: DOI: 10.1002/anie.201601026

Monitoring the Glutathione Redox Reaction in Living Human Cells by Combining Metabolic Labeling with Heteronuclear NMR

*Xing Jin[+], Soeun Kang[+], Shinya Tanaka, and Sunghyouk Park**

Abstract: *The glutathione (GSH) redox reaction is critical for defense against cellular reactive oxygen species (ROS). However, direct and real-time monitoring of this reaction in living mammalian cells has been hindered by the lack of a facile method. Herein, we describe a new approach that exploits the GSH biosynthetic pathway and heteronuclear NMR. [U-^{13}C]-labeled cysteine was incorporated into GSH in U87 glioblastoma cells, and the oxidation of GSH to GSSG by a ROS-producing agent could be monitored in living cells. Further application of the approach to cells resistant to temozolomide (TMZ), an anti-glioblastoma drug, suggested a possible new resistance mechanism involving neutralization of ROS. This result was corroborated by the observation of up-regulation of glutathione peroxidase 3 (GPx3). This new approach could be easily applied to redox-dependent signaling pathways and drug resistance involving ROS.*

Glutathione (GSH) exists at high concentrations (1–11 mM) in cells, mostly in the reduced form,[1] and is critically important for defense against reactive oxygen species (ROS). Oxidation of GSH to the oxidized form (GSSG) with the concomitant reduction of ROS, as mediated by glutathione peroxidase (GPx), is at the heart of this defense system. Since ROS-mediated oxidative stress has been implicated in the pathophysiologies of many diseases, such as cancer, liver diseases, and diabetes mellitus,[2] extensive research has been performed to measure intracellular GSH and GSSG concentrations. Conventional methods involve spectrophotometric determination using dyes such as 5,5′-Dithiobis[2-nitrobenzoic acid] (DTNB)[3] or HPLC.[4] However, these methods require cell lysis for the extraction of GSH and GSSG, during which undesired oxidation of GSH to GSSG could occur. In addition, cell lysis procedures make real-time monitoring of GSH-to-GSSG conversion impossible. Advances in fluorescent probes that can respond to changes in GSH has enabled the detection of GSH in living cells. These approaches include either protein (e.g. Grx1-roGFP)[5] or chemical (e.g. ThiolQuant Green)[6] fluorescent probes; however, all of them are indirect measurements that are susceptible to fluorescence quenching or unequal delivery/expression of probes. More importantly, protein probes require genetic manipulation of the cells, and chemical probes involve the introduction of non-natural molecules into cells, all of which can affect cellular physiology in undesirable and unexpected ways. Alternatively, nuclear magnetic resonance (NMR) techniques, which allow non-destructive measurement,[7] can be suitable for the direct detection of GSH in living cells. A very recent study, in fact, reported direct measurement of GSH in live yeast cells using NMR and exogenously added $^{13}C_2$,^{15}N-glycine-labeled GSH without surrogate probes.[8] However, this approach is limited to only a specially designed mutant yeast strain that imports GSH with a high-affinity transporter and lacks the endogenous GSH biosynthetic machinery to avoid dilution of the labeled GSH. Since these manipulations are not generally applicable to mammalian cells that synthesize GSH,[9] the method is not readily applicable to human cells. Therefore, a means of direct GSH measurement in living mammalian cells, one that can contribute to the investigation of redox status in model systems of human disease, is highly desired. In the present study, we introduce such a system, which involves exploiting the GSH biosynthetic pathways in human cells and real-time 2D heteronuclear NMR. The method is simple and straightforward and can be applied to other cellular disease systems.

To detect GSH directly in mammalian cells, we used [U-^{13}C]-labeled cysteine, which can enter cells and be subsequently converted into γ-Glutamylcysteine (γ-GluCys) and GSH in U87 human brain cancer (glioblastoma) cells (Figure 1 A).[10] Such cysteine-labeled GSH can be selectively and directly detected against other non-labeled peaks by using ^{13}C-isotope-edited heteronuclear single-quantum coherence (HSQC) NMR. One desirable feature of our approach is that the *J*-coupling between the two adjacent ^{13}C atoms of cysteine can be used to unambiguously differentiate GSH synthesized from the added cysteine and pre-existing GSH (Figure 1 B). The cysteine-fed cells were harvested and placed in an NMR tube, and HSQC spectra of the live cells were obtained by using the procedures described in our recent paper[11] in the Supporting Information "Methods" section. We also confirmed that the cells were over 95% viable in the NMR tube after the experiments (Figure S1 in the Supporting Information). The cysteine-labeling approach enabled efficient labeling of GSH in live U87 cells, as shown by the HSQC NMR spectrum (^{1}H $\delta = 2.96$ ppm, ^{13}C $\delta = 28.3$ ppm; Figure 1 C). With the splitting of the signal along the ^{13}C axis (ca. 36 Hz, see inset) owing to the above-mentioned *J*-coupling, and the

[*] X. Jin,[+] S. Kang,[+] Prof. S. Park
College of Pharmacy, Natural Product Research Institute
Seoul National University
1 Gwanak-ro, Gwanak-gu, Seoul, 08826 (Korea)
E-mail: psh@snu.ac.kr
Prof. S. Tanaka
Department of Pathology, Laboratory of Cancer Research, Hokkaido University Graduate School of Medicine
N15, W7, Kita-ku, Sapporo, 060-8638 (Japan)
[+] These authors contributed equally to this work.

Supporting information for this article can be found under: http://dx.doi.org/10.1002/anie.201601026.

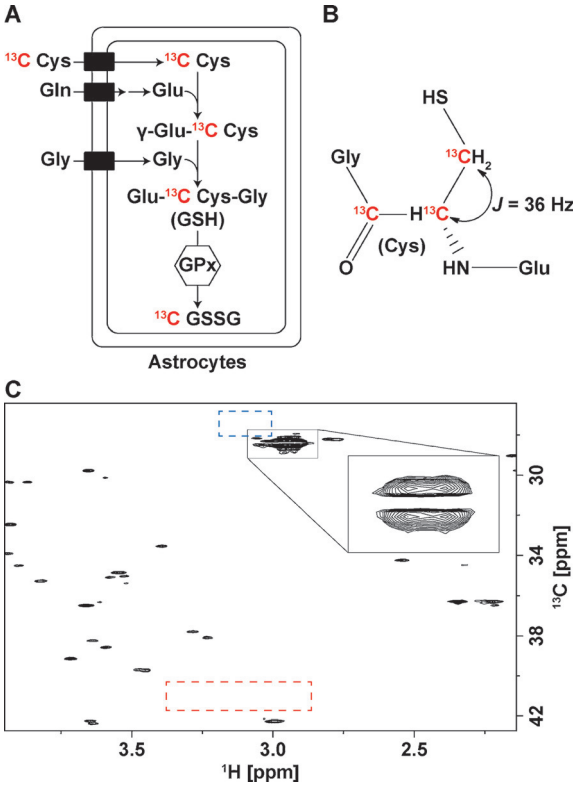

Figure 1. Biosynthetic GSH labeling and its detection by 2D HSQC NMR in live cells. A) The glutathione biosynthetic pathway in human cells. B) *J*-coupling between adjacent ^{13}C atoms in cysteine. C) Intracellular GSH (black box: ^{1}H $\delta = 2.96$ ppm, ^{13}C $\delta = 28.3$ ppm) detected by ^{1}H-^{13}C HSQC NMR in live U87 cells. The black expanded region is for GSH peaks. The blue and red dashed boxes represent the expected peak areas corresponding to cysteine and GSSG, respectively.

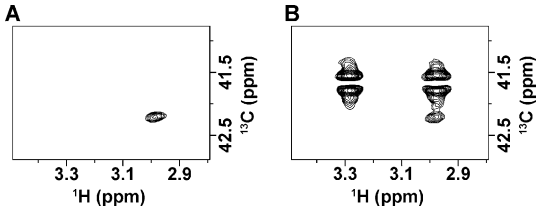

Figure 2. GSSG production monitoring in live U87 cells upon TBH treatment. GSSG in U87 cells without (A) and with (B) 10 mM TBH treatment at the same contour level. The peaks of GSSG peaks corresponding to the beta proton and carbon atom of the cysteine residue are $\delta(^{1}H, ^{13}C) = (2.98, 41.66)$, and (3.29, 41.66) ppm.

low natural abundance of ^{13}C (1%), we could easily detect the GSH synthesized from the added cysteine against the background of GSH signals from the endogenous pool or non-labeled cysteine. In addition, there were no visible signals for the residual cysteine (^{1}H $\delta = 3.05$ ppm, ^{13}C $\delta = 27.8$ ppm) or cystine (^{1}H $\delta = 3.18$ ppm, ^{13}C $\delta = 40.5$ ppm), thus confirming the high efficiency of the labeling approach. The GSSG signals were close to the noise level, which is consistent with the reported physiological ratios between GSH and GSSG in cells (GSH is normally more than 100 times more abundant than GSSG)[12] and the ratio measured using a DTNB-based commercial kit ([GSH]/[GSSG] ≈ 149).

With successful labeling and the observation of the GSH signals from live cells, we tested whether the approach could be used to monitor GSH oxidation by ROS in live cells. We treated U87 cells with *tert*-butylhydroperoxide (TBH),[13] an inducer of intracellular ROS, and monitored the generation of GSSG by ^{1}H-^{13}C HSQC NMR. GSSG, which was close to noise before TBH treatment (Figure 2A), was much increased afterwards (Figure 2B). Again, the splitting pattern along the ^{13}C axis confirmed that the detected GSSG was generated solely from the ^{13}C cysteine-labeled GSH. In addition, we were able to obtain the absolute concentration of GSSG (Figure S2) by using alpha-ketoglutarate as an internal standard, as well as the isotope incorporation ratio (see Methods in the Supporting Information). This demonstrates that our approach can be used to detect ROS-mediated conversion of GSH into GSSG in live cells.

The method was further applied to investigation of the molecular events accompanying resistance in U87 glioblastoma cells to the anticancer drug temozolomide (TMZ), an alkylating agent. This development of resistance is a significant concern in glioblastoma treatment, because TMZ is one of the few anti-glioblastoma drugs.[14] It has generally been believed that an important mechanism of the efficacy of TMZ is DNA methylation and that resistance to TMZ develops through the activity of O^6-methylguanine DNA methyltransferase (MGMT), which reverses the methylation process.[15] However, a very recent study suggested that the therapeutic mechanism of TMZ might also involve oxidative stress and ROS generation.[16] In this case, effective neutralization of ROS would also contribute to the resistance. In terms of the GSH species, ROS neutralization corresponds to the generation of GSSG through GSH oxidation. Therefore, we hypothesized that the ROS-neutralizing mechanism involving the conversion of GSH into GSSG might be more active in TMZ-resistant U87 cells than in their TMZ-sensitive counterparts. We tested this hypothesis by measuring the GSSG levels in both TMZ-resistant U87 (U87R) and TMZ-sensitive parent U87 (U87) cells using our NMR approach. The U87R cells were produced by growing U87 cells in the presence of low concentrations of TMZ (Figure S3).[17] The GSSG levels remained barely detectable regardless of whether the cells were treated with TMZ in the U87 cells, whereas they significantly increased upon TMZ treatment in the U87R cells (Figure 3A). The method also enabled real-time monitoring of the GSSG levels in live cells upon TMZ treatment. The GSSG levels in the U87R cells increased and then returned to a lower level over time upon TMZ treatment, whereas they remained essentially the same in the U87 cells (Figure 3B). Therefore, the resistance of U87R cells to TMZ seems, at least in part, to be related to GSH-to-GSSG oxidation through the reduction of TMZ-generated ROS, which does not operate well in U87 cells. Given that the GSSG levels eventually returned to values close to the pre-treatment values, the U87R cells seemed to possess the ability to maintain redox homeostasis after neutralizing the TMZ-generated ROS. This highlights the importance of real-time detection of GSSG, since a steady-state measurement at time points after around 42 minutes would have missed the initial

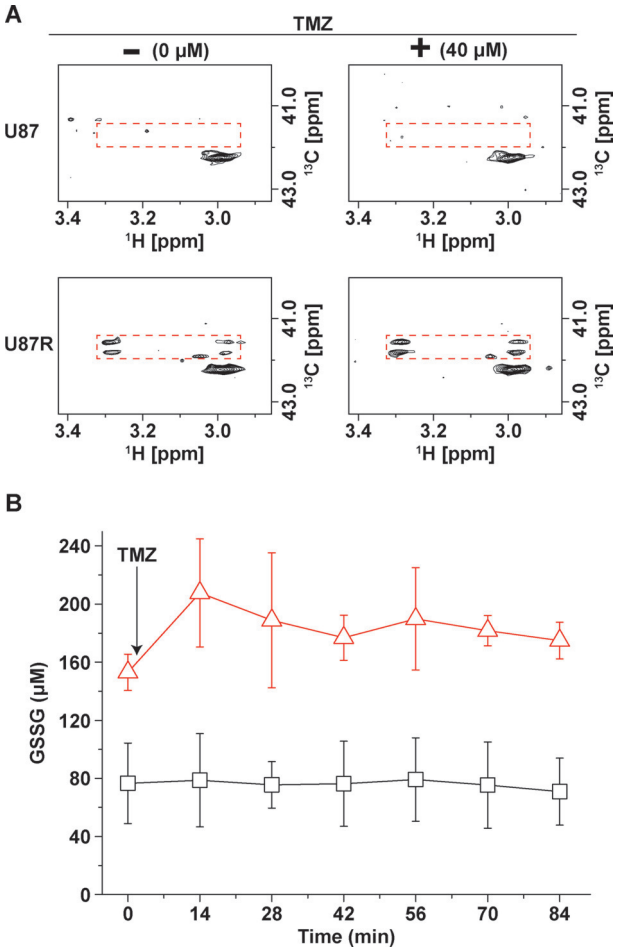

Figure 3. Real-time GSSG changes in U87 and U87R cells following TMZ treatment. A) Comparison of GSSG levels in U87 (upper) and U87R (lower) cells before (left) and after (right) TMZ treatment. The red dashed boxes indicate the GSSG signal regions. B) Real-time monitoring of the GSSG level in U87 (black square) and U87R (red triangle) cells following treatment with 40 μM TMZ. The GSSG concentration was obtained by using alpha-ketoglutarate as an internal control and calibration with LC–MS and cell-volume calculation (see the Supporting Information). The error bars represent standard deviations.

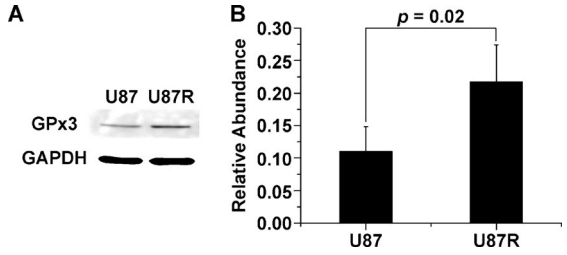

Figure 4. GPx3 expression levels in U87 and U87R cells. A) Western blots for glutathione peroxidase 3 (GPx3). Glyceraldehyde 3-phosphate dehydrogenase (GAPDH) was used as a loading control. B) The bars show the mean band intensities of the protein levels normalized to GAPDH, and the error bars represent standard deviations.

increase. The generally higher levels of GSSG in the U87R cells compared to the U87 cells also suggest that U87R cells are more active in neutralizing ROS with the generation of GSSG. This more-efficient reduction of ROS is consistent with the more-negative glutathione redox potentials of U87R cells than U87 cells, as measured by both our NMR method and a DTNB-based commercial kit (Figure S4).

We next further explored the mechanistic aspect of the enhanced production of GSSG in U87R cells. We measured the enzyme level of glutathione peroxidase (GPx), which is involved in the production of GSSG from GSH accompanied by reduction of ROS. Since glutathione peroxidase 1 (GPx1) is the most well-known GPx isotype, we measured its mRNA levels in U87 and U87R cells by real-time PCR. However, the cells did not exhibit statistically different levels of the enzyme ($p = 0.21$; Figure S5). While searching the literature for a particular GPx isotype that might be responsible for drug resistance, we found a study showing that resistance to cisplatin, an anticancer drug with an ROS-related cytotoxic mechanism, can develop when GPx3 is upregulated.[18] Therefore, we measured the expression levels of GPx3 in U87 and U87R cells and found that it was much more highly expressed in U87R than in U87 cells (Figure 4). This result strongly suggests that more-efficient ROS detoxification by GPx3, and the concurrent oxidation of GSH to GSSG contributes to the resistance of U87 cells to TMZ. This drug-resistance mechanism of ROS neutralization actually has been reported for other DNA-targeting anticancer drugs such as cisplatin and doxorubicin.[18,19] Although the detailed therapeutic mechanism differs between these drugs, with cisplatin being a DNA-crosslinking agent and doxorubicin a DNA-intercalating reagent, they share downstream effects of ROS generation. Therefore, the DNA-alkylating TMZ might also share a similar resistance mechanism despite the difference in its therapeutic DNA-targeting mechanism.

In conclusion, we developed an easy and generally applicable approach for direct estimation of GSH oxidation in live human cells by using biosynthetic cysteine incorporation and heteronuclear NMR. This method was applied to finding a possible new mechanism of TMZ resistance in brain cancer cells. Our approach can be easily extended to other types of drug resistance involving ROS, as well as many signaling pathways modulated by cellular redox status.

Acknowledgements

The research was supported by grants from the Basic Science Research Program through the National Research Foundation of Korea (NRF) funded by the Ministry of Education, Science and Technology (2014M3A9B6069340), from the National R&D Program for Cancer Control (1420290), and from Korean Health Technology R&D Project, Ministry of Health & Welfare, Republic of Korea (Grant HI13C0015), and from the Bio-Synergy Research Project (NRF-2015M3A9C4075818) of the Ministry of Science, ICT and Future Planning through the National Research Foundation.

Keywords: cancer · drug resistance · glutathione · in-cell NMR · redox chemistry

How to cite: *Angew. Chem. Int. Ed.* **2016**, *55*, 7939 – 7942
Angew. Chem. **2016**, *128*, 8071 – 8074

[1] A. Pastore, G. Federici, E. Bertini, F. Piemonte, *Clin. Chim. Acta* **2003**, *333*, 19 – 39.
[2] a) N. Houstis, E. D. Rosen, E. S. Lander, *Nature* **2006**, *440*, 944 – 948; b) T. P. Szatrowski, C. F. Nathan, *Cancer Res.* **1991**, *51*, 794 – 798; c) L. Cesaratto, C. Vascotto, S. Calligaris, G. Tell, *Ann. Hepatol.* **2004**, *3*, 86 – 92.
[3] I. Rahman, A. Kode, S. K. Biswas, *Nat. Protoc.* **2006**, *1*, 3159 – 3165.
[4] G. P. McDermott, P. S. Francis, K. J. Holt, K. L. Scott, S. D. Martin, N. Stupka, N. W. Barnett, X. A. Conlan, *Analyst* **2011**, *136*, 2578 – 2585.
[5] M. Gutscher, A. L. Pauleau, L. Marty, T. Brach, G. H. Wabnitz, Y. Samstag, A. J. Meyer, T. P. Dick, *Nat. Methods* **2008**, *5*, 553 – 559.
[6] X. Jiang, Y. Yu, J. Chen, M. Zhao, H. Chen, X. Song, A. J. Matzuk, S. L. Carroll, X. Tan, A. Sizovs, N. Cheng, M. C. Wang, J. Wang, *ACS Chem. Biol.* **2015**, *10*, 864 – 874.
[7] J. S. Cohen, R. C. Lyon, P. F. Daly, *Methods Enzymol.* **1989**, *177*, 435 – 452.
[8] S. Y. Rhieu, A. A. Urbas, D. W. Bearden, J. P. Marino, K. A. Lippa, V. Reipa, *Angew. Chem. Int. Ed.* **2014**, *53*, 447 – 450; *Angew. Chem.* **2014**, *126*, 457 – 460.
[9] R. Franco, O. J. Schoneveld, A. Pappa, M. I. Panayiotidis, *Arch. Physiol. Biochem.* **2007**, *113*, 234 – 258.
[10] G. Shanker, J. W. Allen, L. A. Mutkus, M. Aschner, *Brain Res.* **2001**, *902*, 156 – 163.
[11] H. Wen, Y. J. An, W. J. Xu, K. W. Kang, S. Park, *Angew. Chem. Int. Ed.* **2015**, *54*, 5374 – 5377; *Angew. Chem.* **2015**, *127*, 5464 – 5467.
[12] O. Zitka, S. Skalickova, J. Gumulec, M. Masarik, V. Adam, J. Hubalek, L. Tmkova, J. Kruseova, T. Eckschlager, R. Kizek, *Oncol. Lett.* **2012**, *4*, 1247 – 1253.
[13] Kanupriya, D. Prasad, M. Sai Ram, R. C. Sawhney, G. Ilavazhagan, P. K. Banerjee, *Toxicol. In Vitro* **2007**, *21*, 846 – 854.
[14] R. Stupp, M. Brada, M. J. van den Bent, J. C. Tonn, G. Pentheroudakis, *Ann. Oncol.* **2014**, *25*, iii93 – iii101.
[15] a) G. J. Kitange, B. L. Carlson, M. A. Schroeder, P. T. Grogan, J. D. Lamont, P. A. Decker, W. Wu, C. D. James, J. N. Sarkaria, *Neuro-Oncology* **2009**, *11*, 281 – 291; b) M. E. Hegi, A. C. Diserens, T. Gorlia, M. F. Hamou, N. de Tribolet, M. Weller, J. M. Kros, J. A. Hainfellner, W. Mason, L. Mariani, J. E. Bromberg, P. Hau, R. O. Mirimanoff, J. G. Cairncross, R. C. Janzer, R. Stupp, *N. Engl. J. Med.* **2005**, *352*, 997 – 1003.
[16] L. Chen, X. Li, L. Liu, B. Yu, Y. Xue, Y. Liu, *Oncol. Rep.* **2015**, *33*, 1465 – 1474.
[17] S. Kohsaka, L. Wang, K. Yachi, R. Mahabir, T. Narita, T. Itoh, M. Tanino, T. Kimura, H. Nishihara, S. Tanaka, *Mol. Cancer Ther.* **2012**, *11*, 1289 – 1299.
[18] Y. Saga, M. Ohwada, M. Suzuki, R. Konno, J. Kigawa, S. Ueno, H. Mano, *Oncol. Rep.* **2008**, *20*, 1299 – 1303.
[19] S. Furusawa, E. Kimura, S. Kisara, S. Nakano, R. Murata, Y. Tanaka, S. Sakaguchi, M. Takayanagi, Y. Takayanagi, K. Sasaki, *Biol. Pharm. Bull.* **2001**, *24*, 474 – 479.

Received: January 29, 2016
Revised: March 18, 2016
Published online: May 12, 2016

